RSC Advances

PAPER

View Article Online
View Journal | View Issue

Cite this: *RSC Adv.*, 2016, **6**, 51286

Experimental determination and model correlation for the solubilities of trialkyl phosphates in supercritical carbon dioxide

K. C. Pitchaiah,[a] N. Sivaraman,*[a] Neha Lamba[b] and Giridhar Madras[b]

Received 27th April 2016
Accepted 19th May 2016

DOI: 10.1039/c6ra10897k

www.rsc.org/advances

The solubilities of a series of trialkyl phosphates in supercritical carbon dioxide have been investigated. The solubility measurement was carried out using a dynamic flow method. The measurements were performed at 313, 323 and 333 K and in the pressure range of 10 to 25 MPa. The trialkyl phosphates were found to be highly soluble in supercritical carbon dioxide and the solubilities were in the range of 0.01 to 0.1 mol fraction. The solubility of trialkyl phosphates increases with an increase in pressure at constant temperature. A reverse behavior was observed, wherein the solubilities decreased with increase in temperature in the investigated pressure region. At constant temperature and pressure, the solubilities of the trialkyl phosphates decrease with the alkyl chain length. The solubility data was found to be consistent with the Mendez–Teja model. The solubilities were correlated by the Chrastil model and an association model based on the van Laar activity coefficient model with absolute deviations of less than 10%. A key result is that the model parameters based on the association model varied linearly with the carbon number.

1. Introduction

Supercritical Fluid Extraction (SFE) of metal ions from diverse matrices is considered as an environmentally friendly alternative to conventional solvent extraction. SFE is an attractive technique for nuclear applications because it can minimize the amount of liquid waste generation. Supercritical fluids have many interesting properties such as liquid-like densities, high diffusivity, low viscosity and low surface tension.[1,2] CO_2 is a widely used supercritical fluid and is considered as a green solvent. It has moderate critical constants and it is also inexpensive, non-flammable, non-toxic and easily recyclable. Supercritical carbon dioxide ($SCCO_2$) has several applications in material synthesis and processing[3] and it is also used as a solvent for the extraction of non-polar and moderately polar compounds.[2] Extraction of metal ions using neat CO_2 is not possible because of its weak solute–solvent interactions and charge neutralization.[4,5] However, metal ion extraction can be achieved by complexing them with suitable ligands and the resultant metal complex could become quite soluble in $SCCO_2$.[4,6] The extraction behavior mainly depends on the (a) solubility of ligand/complexing agent and (b) solubility and stability of the resultant metal-complex in $SCCO_2$.[7] The primary criterion for the use of a ligand in SFE is that it should have appreciable solubility in $SCCO_2$. Therefore, the solubility of ligand as well as that of metal complex plays a crucial role in designing and optimization of a SFE process.

The organophosphorus compounds contain the phosphoryl group that is used in the extraction and purification of various metal ions in chemical and hydrometallurgical industries. Extraction of actinides from acidic waste solutions is an important task in nuclear waste management that can reduce the radiological burden of the waste. Neutral organophosphorus compounds such as phosphates, phosphonates, phosphinates and phosphine oxides have been used for solvent extraction of metal ions for the extraction and recovery of actinides from liquid and solid matrices.[8–10] These compounds have wide range of applications in nuclear industry from mining of nuclear materials to reprocessing of the spent nuclear fuel. The extraction power of these molecules was found to be increasing in the order: phosphates < phosphonates < phosphinates < phosphine oxides.[11] Among these, trialkyl phosphate based molecules have been used for the metal ion extraction.[12] Further, among trialkyl phosphates, tributyl phosphate (TBP) is widely used as an extractant in various steps of nuclear fuel reprocessing.[13,14] A wide range of other trialkyl phosphates such as triisobutyl phosphate (TiBP), triisoamyl phosphate (TiAP), triamyl phosphate (TAP) and trihexyl phosphate (THP) have also examined for the extraction of actinides.[15–17] SFE of metal ions such as heavy metals, lanthanides and actinides from different matrices using organophosphorus compounds was carried out.[4,5,7,18,19] SFE based methods were developed for the

[a]*Chemistry Group, Indira Gandhi Centre for Atomic Research, Kalpakkam-603102, India. E-mail: sivaram@igcar.gov.in; Fax: +91-044-27480065; Tel: +91-044-27480500-24166*

[b]*Department of Chemical Engineering, Indian Institute of Science, Bangalore-560012, India*

extraction of actinides from various matrices with organophosphorus compounds.[20–24]

The determination of solubility of organophosphorus ligands in $SCCO_2$ is crucial towards designing a SFE method for recovery of a metal ion. The solubility of a variety of complexing agents and metal complexes in $SCCO_2$ has been reviewed.[25–30] However, the literature on the solubilities of organophosphorus compounds in $SCCO_2$ is scarce. The solubilities of TBP,[27,31] triphenyl phosphate (TPP), triphenyl phosphine (TPPh), triphenyl phosphine oxide (TOPO) and other paraffinic hydrocarbon have already been determined.[30] But the solubility behavior of other trialkyl phosphates has not been studied.

The experimental determination of solubilities of compounds in supercritical fluid (SCF) is difficult and time consuming. Mathematical models have been used to correlate the solubility data.[32] There are certain types of models such as equation of state based models, neural network models[33–35] and semi-empirical models that can be used to correlate and predict the solubilities of compounds in SCF. The equation of state based models require the knowledge of pure component properties that are not readily available and require group contribution theory methods.[32,36] Similarly, neural network models has a disadvantage of time requirement to train the nets.[37] Thus, empirical or semi-empirical models are preferably used for solubility determination. Several empirical models are available in the literature.[38–47] Density based models are the most commonly used semi-empirical equations. Many of these models correlate the solubilities of solids. However, the models that correlate the solubility of liquid solutes in supercritical fluids are scarce. A semi-empirical equation for correlating the liquid solubilities in supercritical fluids based on solution theory coupled with Wilson activity coefficient model was developed.[48] Recently, several correlations based on association/solution theories using different activity coefficients have been developed.[49]

The solubilities of various trialkyl phosphates in $SCCO_2$ were experimentally determined at different temperatures and pressures. These solubilities were correlated with various semi-empirical correlations such as the Chrastil,[38] Méndez-Santiago and Teja[43] models. The solubilities were also correlated by a recently developed association model based on van Laar activity coefficient.[50] A key result found in this study was that the model parameters of the association model based on van Laar activity coefficient varied linearly with the carbon number of the trialkyl phosphates.

2. Experimental

2.1. Materials

Carbon dioxide with a purity of 99.9% was used for the solubility measurements. Trimethyl phosphate (TMP) (Koch Light Laboratories Ltd.), triethyl phosphate (TEP) (99%, Sigma Aldrich) and tributyl phosphate (TBP) (99%, Alfa), were used as such without any purification. The compounds, triamyl phosphate (TAP) and trihexyl phosphate (THP) were synthesized by the condensation reaction between $POCl_3$ and stoichiometric equivalent of corresponding alcohol in the presence of pyridine with *n*-heptane as the reaction medium.[16] TAP and THP were purified by vacuum distillation followed by washing with concentrated sodium hydroxide and water. The characterization of TAP and THP was carried out using infrared (IR) spectroscopy, elemental analysis and ^{31}P NMR. The purity of these compounds was determined by gas chromatography (GC) with flame ionization detector (FID) and the purity was found to be ~99%. All other chemicals used were of analytical grade.

2.2. Procedure

The schematic of continuous flow apparatus used in this study for measuring the solubility in supercritical carbon dioxide is shown in Fig. 1. The experimental setup consisted of a carbon dioxide cylinder (1), a high pressure reciprocating CO_2 pump (JASCO-PU-2080-CO_2) (3), 10 mL CO_2 tank (6), 50 mL twin high pressure equilibrium cells (7 & 8), thermostat (JASCO-CO-156) (10), and a back pressure regulator (JASCO-880-81-BP) (11). The uncertainties in the temperature and pressure measurements are ±0.1 K and ±0.1 MPa, respectively.

An appropriate amount of trialkyl phosphate was loaded into the equilibrium cells (7 & 8). The outlet of the first vessel (7) was connected as inlet for the second vessel (8). The saturated carbon dioxide stream from the second vessel (8) flows through an entrainer column (9) that traps the entrained liquid. Two equilibrium cells and entrainer column were placed in a thermostat (10) to maintain a constant temperature. The system pressure was regulated and controlled by a back pressure regulator.

Carbon dioxide from the gas cylinder (1) was passed through a silica gel column (2) to remove traces of water and then fed into a CO_2 pump (3) where it was liquefied by using a Peltier element. Liquid carbon dioxide was pressurized and sent to the CO_2 tank (6) placed inside the thermostat to reach the supercritical state prior to its entry into the equilibrium cells (7 & 8). At a fixed experimental temperature, the equilibrium cells were pressurized with $SCCO_2$ until the desired pressure was reached. The system was kept at the desired temperature and pressure for an hour to reach the equilibrium. After equilibration, $SCCO_2$ was allowed continuously to flow through the system at

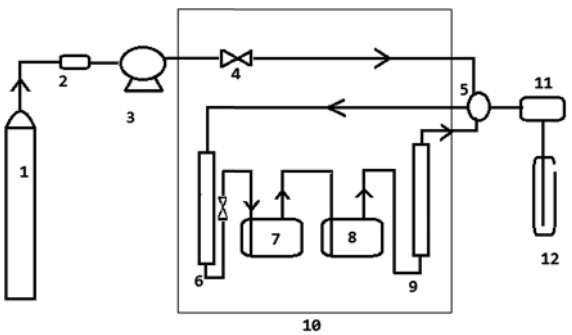

Fig. 1 Schematic of the experimental set-up used for the solubility measurements. (1) CO_2 cylinder, (2) silica column, (3) high pressure CO_2 pump, (4) valve, (5) six way valve, (6) CO_2 tank/heat exchanger, (7 & 8) twin equilibrium cells (9) entrainment column, (10) thermostat, (11) back pressure regulator, (12) collection vessel.

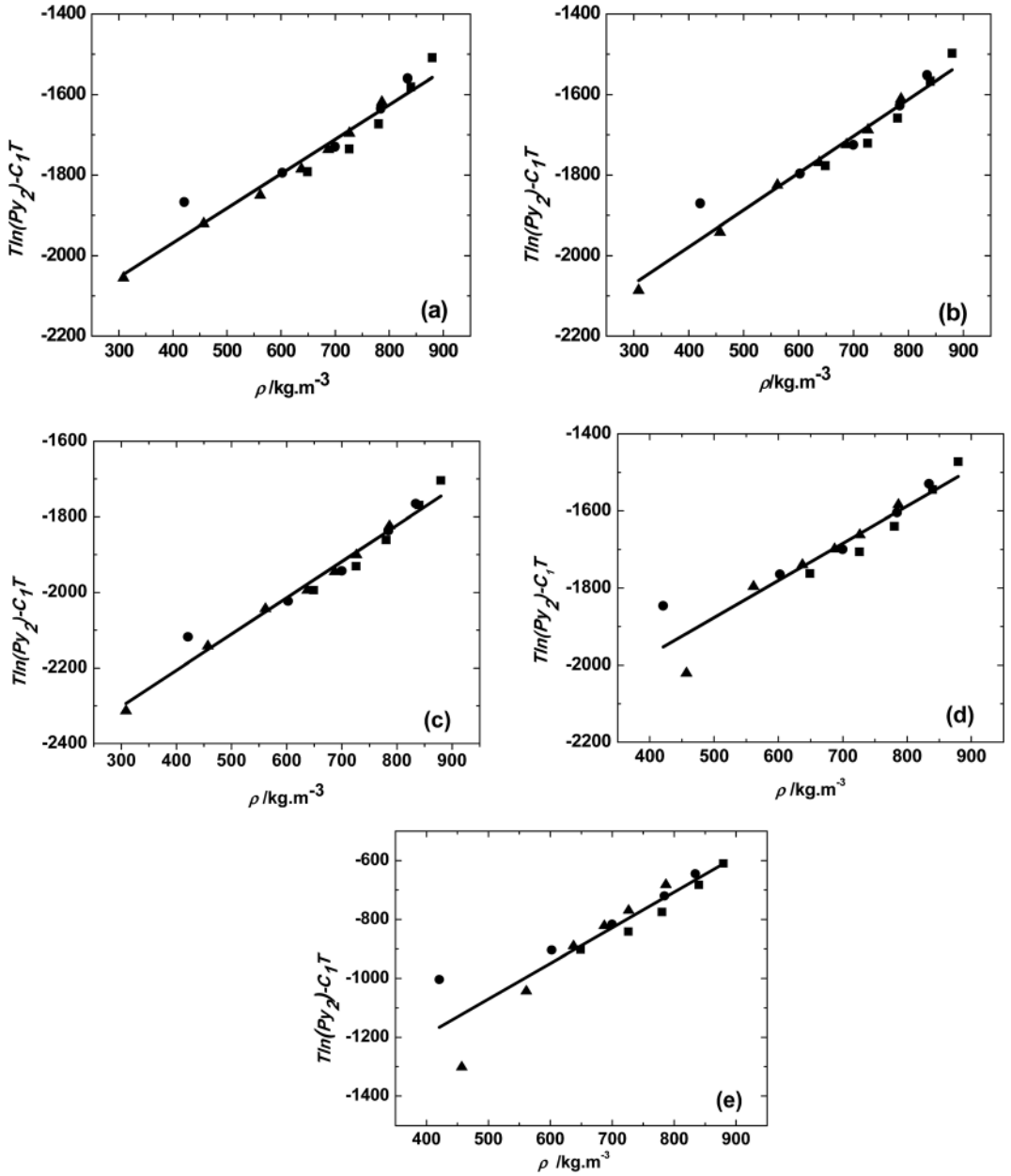

Fig. 2 Solubility of (a) trimethyl phosphate, (b) triethyl phosphate, (c) tributyl phosphate, (d) triamyl phosphate, (e) trihexyl phosphate at different temperatures, ■, 313 K; ●, 323 K; ▲, 333 K. Solid line represents the MT model fit (eqn (3)).

a constant flow rate and the concentration of solute in the $SCCO_2$ stream was monitored continuously. The exiting CO_2 stream from equilibrium cells was introduced into a collection vessel (12), where the pressure was reduced to atmospheric pressure. Saturation solubility was achieved and it was observed by periodically collecting the solute and quantifying the same. It was found that the solubility did not vary with the time and outlet CO_2 stream was saturated with the solute, which ensures the equilibrium.

The primary criterion for the accurate measurement of solubilities in $SCCO_2$ is that the exiting stream has to be saturated with the solute. Repeated measurements were carried out at different flow rates of CO_2 between 0.1 and 1 mL min^{-1}, to ensure saturation of solute in $SCCO_2$ medium. It was found that the solubilities did not vary with flow rates up to 0.3 mL min^{-1}. When the flow rate was increased beyond 0.4 mL min^{-1}, the concentration of solute in the exiting stream decreased with the flow rate, indicating that the exiting stream has not been saturated with the solute. Hence, a CO_2 flow rate of 0.1 mL min^{-1} was employed to ensure that the exiting CO_2 was saturated with the trialkyl phosphate. The exiting stream was trapped and collected in collection vessel containing *n*-hexane, at regular intervals of time. Subsequently, *n*-hexane was evaporated and the amount of solute collected was determined gravimetrically using an analytical balance (±0.1 mg). However, quartz wool was also used as a trap to collect the

Table 1 Experimental solubilities of trialkyl phosphates in $SCCO_2$ as a function of temperature and pressure

			Solubility y_2 (mol mol^{-1})				
T (K)	P (MPa)	Density[a] (kg m^{-3})	TMP	TEP	TBP	TAP	THP
313	8.3	320.54	0.188	0.160	0.105	0.097	0.075
	10.3	651.49	0.191	0.162	0.110	0.099	0.081
	12.3	727.57	0.191	0.163	0.113	0.099	0.082
	15	781.32	0.192	0.163	0.116	0.101	0.083
	20	840.61	0.193	0.163	0.117	0.102	0.084
	25	880.15	0.194	0.163	0.115	0.103	0.085
323	10.3	423.74	0.180	0.145	0.092	0.091	0.065
	12.3	604.62	0.189	0.152	0.103	0.098	0.074
	15	701.08	0.190	0.156	0.108	0.098	0.079
	20	785.16	0.191	0.158	0.113	0.099	0.080
	25	834.89	0.192	0.160	0.113	0.100	0.081
333	10.3	309.89	0.122	0.090	0.062	0.014	0.005
	12.3	458.89	0.153	0.116	0.087	0.054	0.024
	14	563.09	0.165	0.144	0.102	0.092	0.046
	16	638.84	0.177	0.150	0.104	0.096	0.064
	18	688.34	0.182	0.153	0.107	0.096	0.070
	20	724.63	0.185	0.154	0.110	0.097	0.074
	25	787.28	0.186	0.155	0.111	0.098	0.077

[a] Density values taken from http://www.webbook.nist.gov/chemistry/fluid/

solute in the collection vessel and the collection efficiency was found to be similar to that of *n*-hexane. The precision of the gravimetric determination was 0.5%. The reliability of the experimental set-up and procedures were tested by measuring the solubility of tributyl phosphate and trioctyl amine in $SCCO_2$ medium. The results were in good agreement with the literature data.[25,27]

The mole fraction solubility (y_2) and solubility in g L^{-1} (S) is calculated using the expressions

$$y_2 = \frac{n_2}{f \times t \times \rho_1 + n_2} \quad (1)$$

$$S = \frac{\left(\frac{W}{M_w}\right) \times 1000}{(f \times t \times \rho_1) + (W \times \rho_2^{-1})} \quad (2)$$

In eqn (1) and (2), n_2 is number of moles of compound collected, f is the flow rate in mL min^{-1} of the CO_2 at CO_2 pump, t represents the collection time in min and ρ_1 gives the molar density of CO_2 at pump head, W is the amount of compound collected in g, M_w is the molecular weight of the compound and ρ_2 is the density of the compound at experimental temperature.

The solubilities were measured three times at each experimental conditions. The uncertainty of experimental measurements was found to be ±5%. The density data used in this study was from NIST Web Book.

3. Models and correlations

3.1. Méndez–Teja (MT) model

Méndez-Santiago and Teja[43] derived an expression that can be used for checking the consistency of the experimental data of solubility of solutes in supercritical carbon dioxide. This model represents the solubility in terms of temperature, pressure and density as

$$T \ln(Py_2) = A_1 + B_1\rho + C_1T \quad (3)$$

In eqn (3), y_2 is the solubility in mol mol^{-1}, P is the pressure in MPa, T is the temperature in K and A_1, B_1 and C_1 are the temperature independent constants. Thus a plot of $T \ln(Py_2) - C_1T$ and ρ would be linear with all the isotherms collapsing on to a single straight line.

Table 2 Regression analysis and model parameters for the correlation of solubilities of trialkyl phosphates by Chrastil model (eqn (3)), MT model (eqn (4)) and the association model based on van Laar activity coefficient model (eqn (7))

Model	Model Parameters	TMP	TEP	TBP	TAP	THP
MT model	A_1	−2313 ± 36	−2358 ± 35	−2593 ± 30	−2363 ± 60	−2052 ± 60
	B_1	0.85 ± 0.05	0.92 ± 0.05	0.96 ± 0.04	0.97 ± 0.08	0.94 ± 0.08
	C_1	6.4 ± 0.5	6.26 ± 0.5	6.54 ± 0.54	5.7 ± 0.5	4.54 ± 0.4
	R^2	0.942	0.954	0.967	0.885	0.913
	AARD (%)	7	7	6	9	10
Chrastil model	A_2	−1.56 ± 0.01	−1.75 ± 0.02	−1.50 ± 0.01	0.53 ± 0.02	−1.84 ± 0.01
	B_2	514 ± 4	433 ± 4	392 ± 4	106 ± 1	546 ± 3
	k	0.890 ± 0.03	0.957 ± 0.04	0.929 ± 0.01	0.758 ± 0.01	0.896 ± 0.01
	R^2	0.937	0.954	0.968	0.997	0.973
	AARD (%)	6	7	5	3	4
Association model based on van Laar activity coefficient model	k_{VL}	1	1	1	1	1
	A_{VL}	2369 ± 27	3169 ± 40	4400 ± 150	5520 ± 105	6250 ± 150
	C_{VL}	−3295 ± 18	−3885 ± 23	−5192 ± 27	−6110 ± 61	−6980 ± 48
	D_{VL}	−118 ± 5	−176 ± 5	−289 ± 6	−376 ± 12	−390 ± 20
	E_{VL}	10.9 ± 0.4	13 ± 0.1	17.8 ± 0.6	21 ± 1.2	24 ± 0.8
	F_{VL}	−9.3 ± 0.1	−12.1 ± 0.12	−16.6 ± 0.13	−20.3 ± 0.4	−23 ± 0.5
	R^2	0.90	0.87	0.92	0.70	0.84
	AARD (%)	3	3	3	7	5

3.2. Chrastil model

The Chrastil model[38] relates the solubility of solute and density of the pure supercritical fluid (SCF) as follows

$$\ln(S) = k\ln(\rho) + \frac{A_2}{T} + B_2 \quad (4)$$

In eqn (4), S is the solubility of solute in SCF in g L^{-1}; ρ is the density of the SCF in g L^{-1}; k is the association number that describes the number of solvent molecules associated with the complex; A_2 is a function of enthalpy of vaporization and enthalpy of solvation; T is the temperature in K; B_2 depends on the association number and molecular weight of solute and supercritical fluid. Thus a plot of $\ln(S)$ with $\ln(\rho)$ will be linear at a constant temperature.

3.3. Association model with van Laar activity coefficient model

An association model, such that a molecule of solute A (liquid) associates with k molecules of solvent B ($SCCO_2$) to form a solvate complex, AB_k was developed[50] with the assumption of formation of solvato complex which is in equilibrium with the supercritical phase. An expression in terms of densities of both phases, fugacities, activity coefficients, pressure and temperature was obtained as

$$\ln y_2 = (k-1)\ln\left(\frac{P}{P^*}\right) + \frac{\Delta H_s}{RT} - q_s - \left[2\left(B_{AB_kB} - kB_{BB}\right) + (k-1)B\right]\rho_B - \ln\left(\frac{\phi_B^{*k}}{\phi_{AB_k}^*}\frac{\phi_A^*}{\phi_{sat}}\frac{P^*}{x_A}\right) + A_v - \frac{B_v}{T} + \ln\gamma_A + \frac{\rho_B}{\rho_A} \quad (5)$$

The above expression was simplified and the activity coefficient was modeled using a van Laar activity coefficient model and the following expression was obtained,

$$y_2 = \left(\frac{P}{P^*}\right)^{k_{VL}-1}\exp\left[\left(\frac{1}{T}\right)\left\{A_{VL} + C_{VL}\left(\frac{\rho_B}{\rho_A}\right) + D_{VL}\left(\frac{\rho_B}{\rho_A}\right)^2\right\} + E_{VL}\left(\frac{\rho_B}{\rho_A}\right) + F_{VL}\right] \quad (6)$$

In eqn (6), y is solubility, P is pressure in MPa, P^* is reference pressure, T is temperature in K, ρ_B, ρ_A and x_B, x_A are the molar densities in kg m^{-3} and mole fractions of solvent (B) and solute (A), respectively. k_{VL} represents association number and A_{VL}, B_{VL}, C_{VL}, D_{VL}, $E_{VL}$and F_{VL} are temperature independent constants. Eqn (6) was used for correlating the solubilities of trialkyl phosphates in $SCCO_2$.

4. Results and discussion

The solubilities of various trialkyl phosphates: TMP, TEP, TBP, TAP and THP were measured at temperatures of 313, 323 and 333 K in the pressure range of 10 to 25 MPa. The consistency of the solubility data was checked by the MT model (eqn (3)) as shown in Fig. 2. The constants A_1, B_1, and C_1 in the eqn (3) were obtained by the multiple linear regression of the experimental data and given in Table 2. The plot of $T\ln(Py_2) - C_1T$ and ρ was linear with all experimental data fitting onto single straight line and this indicates that the data is self-consistent.

In general, the solubilities of trialkyl phosphates were found to be high in the investigated region and are shown in Table 1. The variation of solubilities with temperature and pressure is shown in Fig. 3 for different trialkyl phosphates. Across all the isotherms (313, 323 and 333 K) the solubilities of trialkyl phosphates increases with the pressure. We have included the solubility data for TBP from existing literature[27] and compared it with the present data in Fig. 3 and the agreement is reasonable. Increasing the pressure at isothermal conditions increases the density of $SCCO_2$ that improves the specific interactions between CO_2 and solute molecules, enhancing the solvating power and leading to higher solubility. The reverse behavior was observed with temperature and the solubilities of trialkyl phosphates decreases with temperature in the entire pressure region. The effect of temperature on the solubility is not straight forward and there are two competing factors that can influence the solubility. The vapor pressure of the solute generally increases with the temperature whereas density of $SCCO_2$ decreases with increase in temperature.[49] However, the vapor pressure of the trialkyl phosphates in the investigated temperature region of 313 to 333 K is low and hence making density as the dominating factor. The decrease of $SCCO_2$ density with temperature results in reduced solubility at 333 K compared to that obtained at 313 K, as depicted by Fig. 3.

From the solubility data, it was observed that TMP has highest solubility among its homologous series investigated in the present study. The solubilities of TMP ranged from 0.122 to 0.194 mol mol^{-1}. THP has relatively lower solubilities, ranging from 0.005 to 0.085 mol mol^{-1}. All other trialkyl phosphates show intermediate solubility in comparison to TMP and THP. It was found that the solubility is inversely related to the number of carbon atoms present in the trialkyl phosphate. The vapor pressure is a parameter influencing the solubility behavior and is directly dependent on the molecular weight of the compound. For a homologous series, the solubility of a solute decreases with increase in carbon number where generally, the vapor pressure decrease with increase in carbon chain.[51,52] In Fig. 4, experimental solubilities of trialkyl phosphates were plotted against their carbon number at 20 MPa with temperature ranging from 313 to 333 K. It was found that, in the homologous series of trialkyl phosphates, the solubility decreases with its molecular weight or carbon number at all isotherms. The solubility of trialkyl phosphates decreases with increase in the temperature as the density of $SCCO_2$ decreases with the temperature.

The interaction and solubility of trialkyl phosphates in $SCCO_2$ is mainly due to Lewis acid (LA)–Lewis-base (LB) interactions and weak C–H–O hydrogen bonding.[53] Because of large quadrupole moment of CO_2, there will be a charge separation between carbon and oxygen atoms and electron

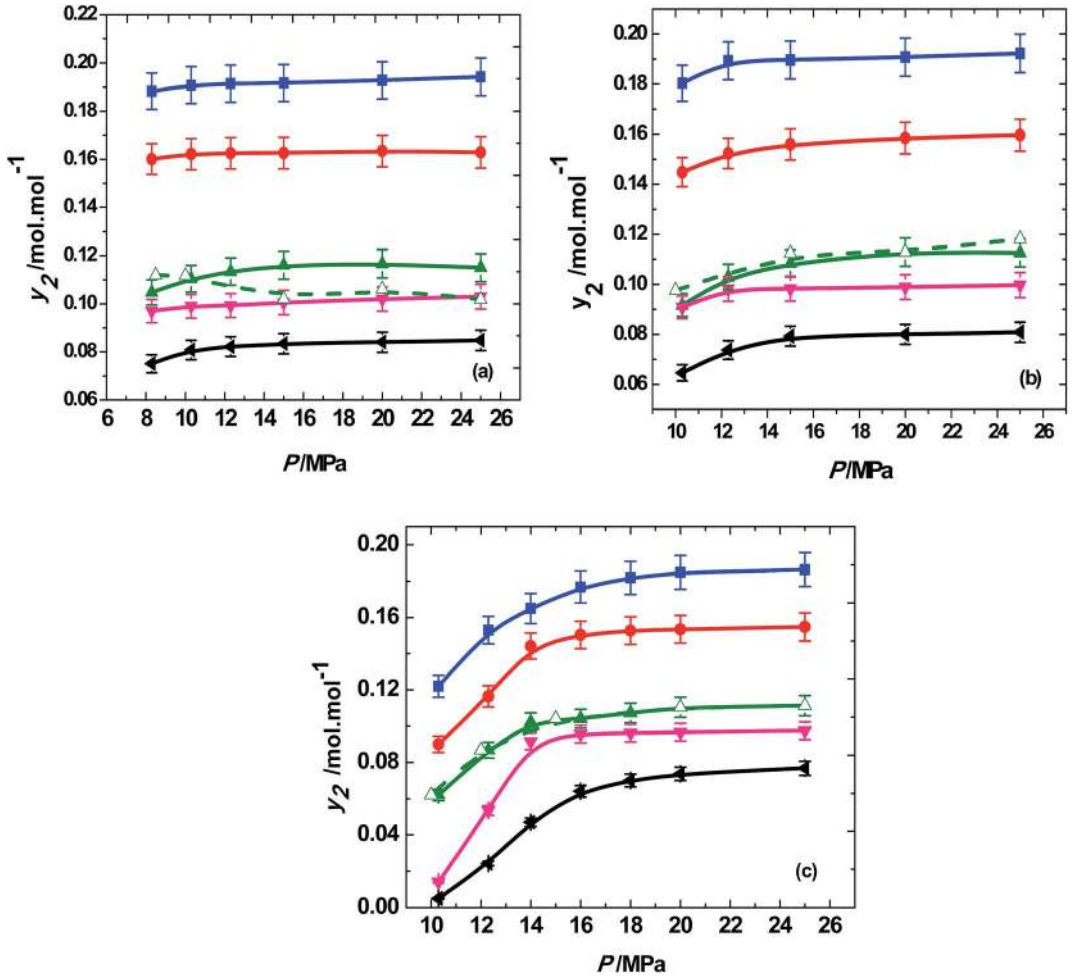

Fig. 3 Variation of solubility of trialkyl phosphates (■, trimethyl phosphate; ●, triethyl phosphate; ▲, tributyl phosphate; ▼, triamyl phosphate; ◄, trihexyl phosphate) with pressure at different temperatures of (a) 313 K; (b) 323 K; (c) 333 K. Solid symbols and solid lines represent the present work. Open symbols and dash line represent the tributyl phosphate (TBP) data by Meguro *et al.*[27]

density moves towards oxygen. Therefore, the carbon atom has partial positive charge acting as a LA and oxygen atoms having negative charge act as a LB. The phosphoryl group of the trialkyl phosphate acts as LB and interacts with the CO_2 through LA–LB interactions.[53] The partial negative charge on oxygen atom induces the electrostatic interaction with –C–H group present in the trialkyl phosphate to form a weak H-bonding. Kim *et al.* performed the quantum mechanical calculations for the CO_2–TMP complex and found that the LA–LB interaction energy was much higher than the weak H-bonding and it could be the main driving force for the higher solubility in CO_2.[53] The high solubilities in the investigated pressure and temperature range may be due to the complete miscibility of the trialkyl phosphates with $SCCO_2$. Meguro *et al.* reported high solubility behavior of TBP in $SCCO_2$ due to the formation of single phase TBP–$SCCO_2$.[27]

Chrastil equation has been employed in the present study to correlate the solubility data of trialkyl phosphates in $SCCO_2$. The experimental solubilities were fitted using non-linear curve fitting with eqn (4) to obtain the model parameters k (association number), A_2 and B_2 and were given in Table 2. The

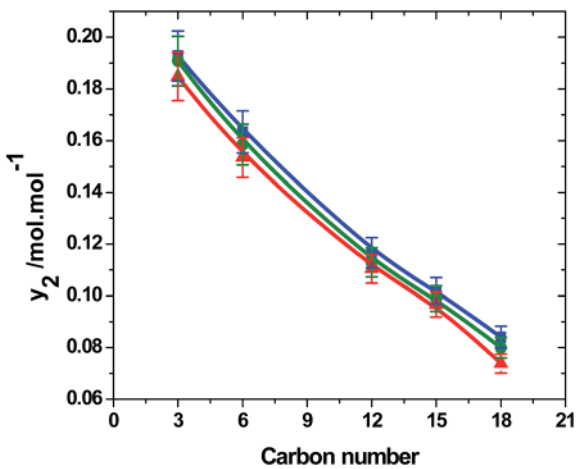

Fig. 4 Variation of solubility of trialkyl phosphates with their carbon number at 20 MPa, with temperatures ■, 313 K; ●, 323 K; ▲, 333 K.

logarithm of solubility (g L^{-1}) data was plotted against the logarithm of density (g L^{-1}) of $SCCO_2$. These plots represent straight lines for different isotherms and are shown in Fig. 5.

The slopes of the different isotherms are close; however, the slope shows a small increase at higher temperature.

Assuming the association number, k_{VL}, to be unity in eqn (6), this equation can be rewritten as,

$$y = \exp\left[\left(\frac{1}{T}\right)\left\{A_{VL} + C_{VL}\left(\frac{\rho_B}{\rho_A}\right) + D_{VL}\left(\frac{\rho_B}{\rho_A}\right)^2\right\} + E_{VL}\left(\frac{\rho_B}{\rho_A}\right) + F_{VL}\right] \quad (7)$$

Eqn (7) was used to determine the solubility by the model and was compared with the experimental solubilities. The model parameters were obtained by non-linear curve fitting and represented in Table 2. The solubilities correlated by the model are depicted by Fig. 6. The deviation of the experimentally measured solubilities from the solubilities derived from the model was estimated by calculating the average absolute relative deviation (AARD%) and is given by eqn (8),

$$\text{AARD\%} = \frac{100}{N}\sum_{i=1}^{N}\left(\frac{|y_{2,cal} - y_{2,exp}|}{y_{2,exp}}\right) \quad (8)$$

$y_{2,cal}$ is the solubility calculated by the model, $y_{2,exp}$ is the experimental solubility and N is the number of data points. The average AARD% obtained from MT, Chrastil and the association

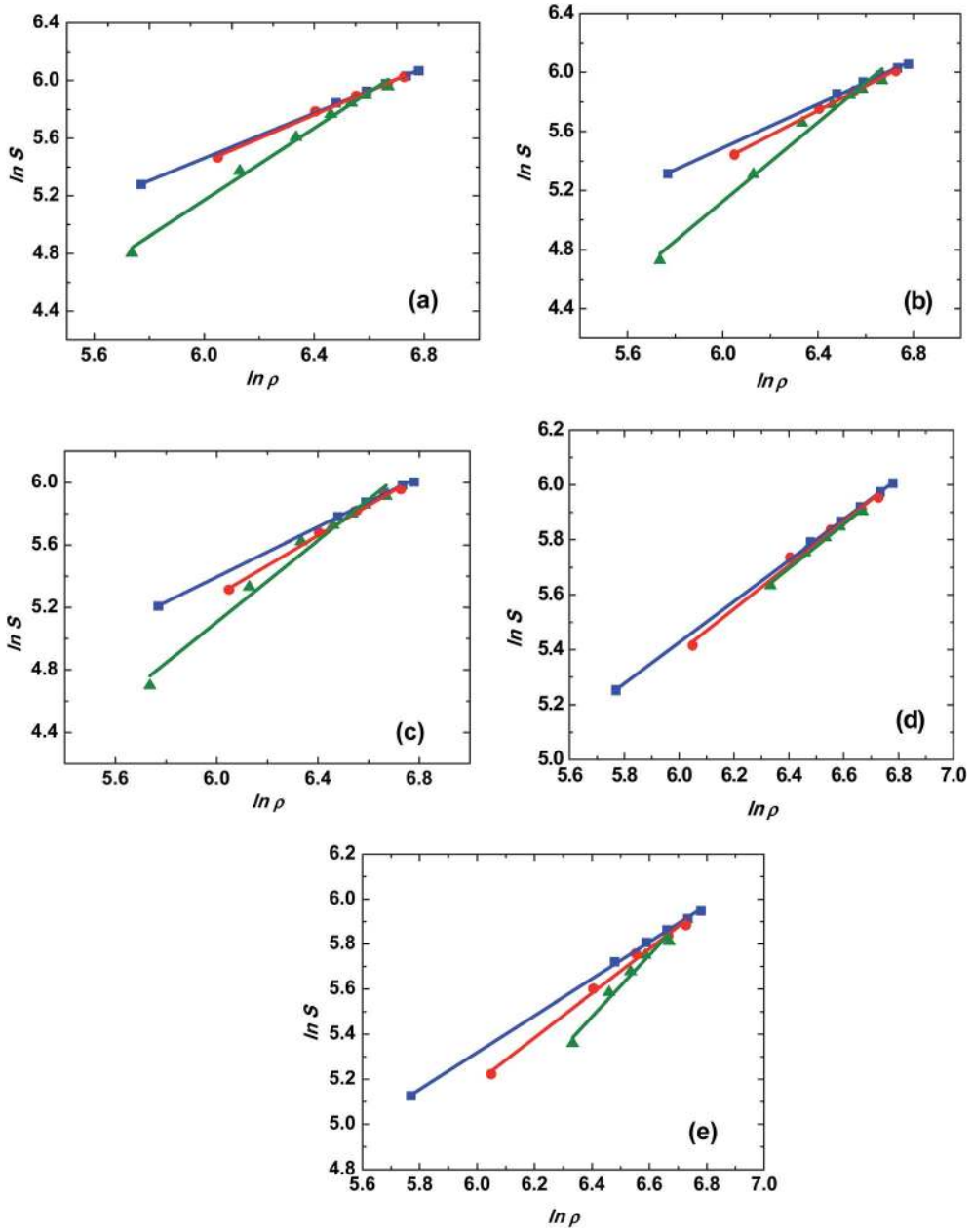

Fig. 5 Correlation plots of ln S *vs.* ln ρ (eqn (4)) for trialkyl phosphates in the pressure range of 10 to 25 MPa, and the temperature of ■, 313 K; ●, 323 K; ▲, 333 K; (a) trimethyl phosphate, (b) triethyl phosphate, (c) tributyl phosphate, (d) triamyl phosphate, (e) trihexyl phosphate.

model based on van Laar activity coefficient are 8%, 5% and 4%, respectively.

While correlating the solubilities of alkanes in supercritical carbon dioxide, it was observed that the adjustable binary interaction parameters in the model vary linearly with the chain length of the *n*-alkanes.[54] Other studies have indicated that the vapor pressure is an important physicochemical parameter influencing the solubility behavior and gives a direct correlation on the solubilities in supercritical fluids.[51] Based on the above observations, the boiling points of the trialkyl phosphates[55,56] were correlated with the carbon number of the trialkyl phosphates. This relationship is linear as observed in the inset of Fig. 7(c). Therefore, the model parameters of the all three models used in the present study were correlated with the carbon number of the trialkyl phosphates. The model parameters of the MT and Chrastil model did not show any particular trend with the carbon number, as shown in Fig. 7(a) and (b). However, the five model parameters of the association model based on van Laar activity coefficient model successfully correlated with the carbon number of the trialkyl phosphates. A linear relationship was observed, as shown in Fig. 7(c). These equations reveal the anticipated trend of solubility with the molecular weight of the trialkyl phosphates. All the three models discussed in this study gave average AARD values ranging from 4% to 8%. However, the association model gave a linear relationship between the model parameters and the carbon number of the trialkyl phosphates. This provides an easy method to calculate the unknown solubilities of other members

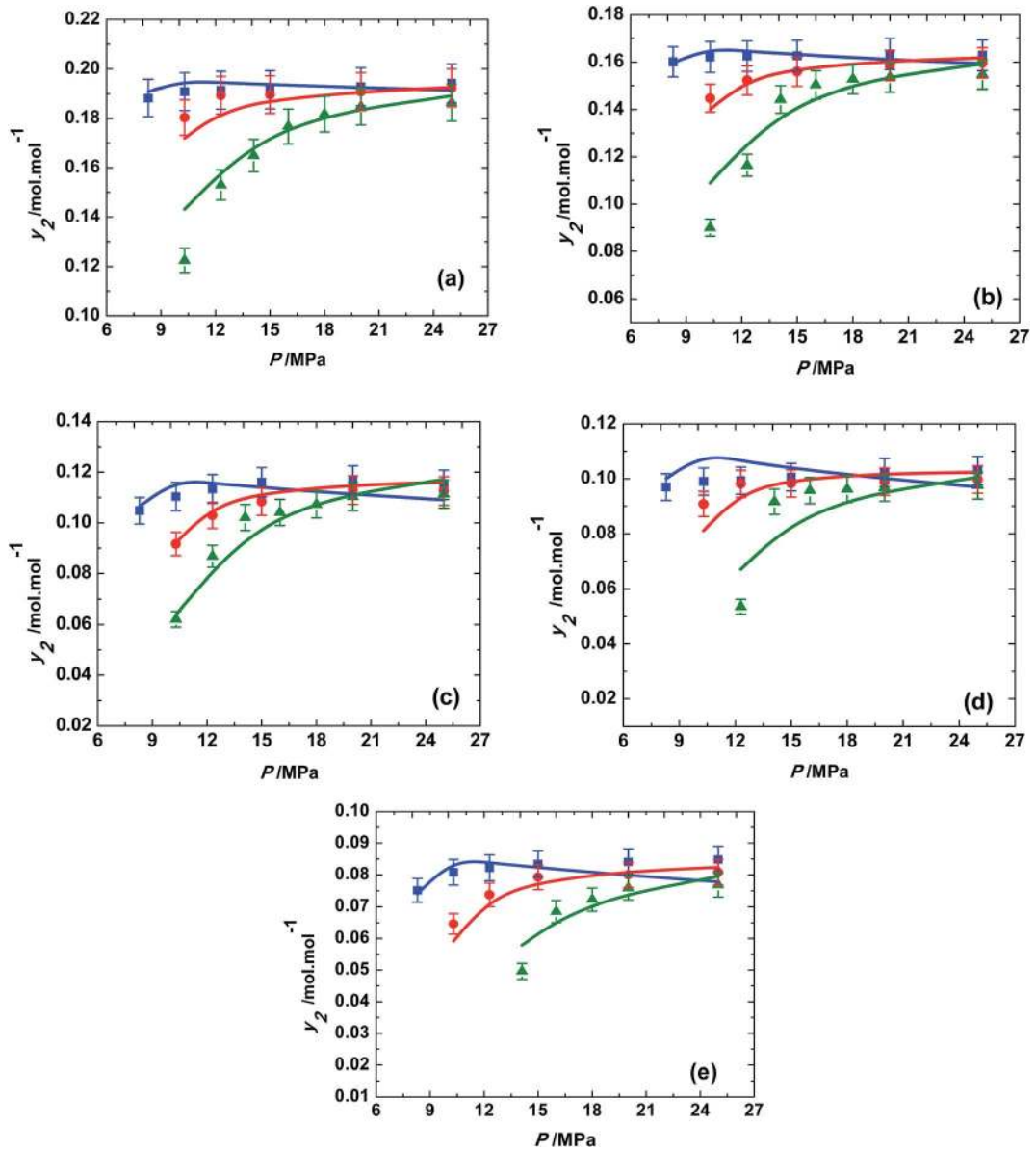

Fig. 6 Variation of solubility of trialkyl phosphates with pressure at different temperatures; ■, 313 K; ●, 323 K; ▲, 333 K; in supercritical carbon dioxide. (a) Trimethyl phosphate, (b) triethyl phosphate, (c) tributyl phosphate, (d) triamyl phosphate, (e) trihexyl phosphate; the solid line represents the association model based on van Laar activity coefficient model (eqn (7)).

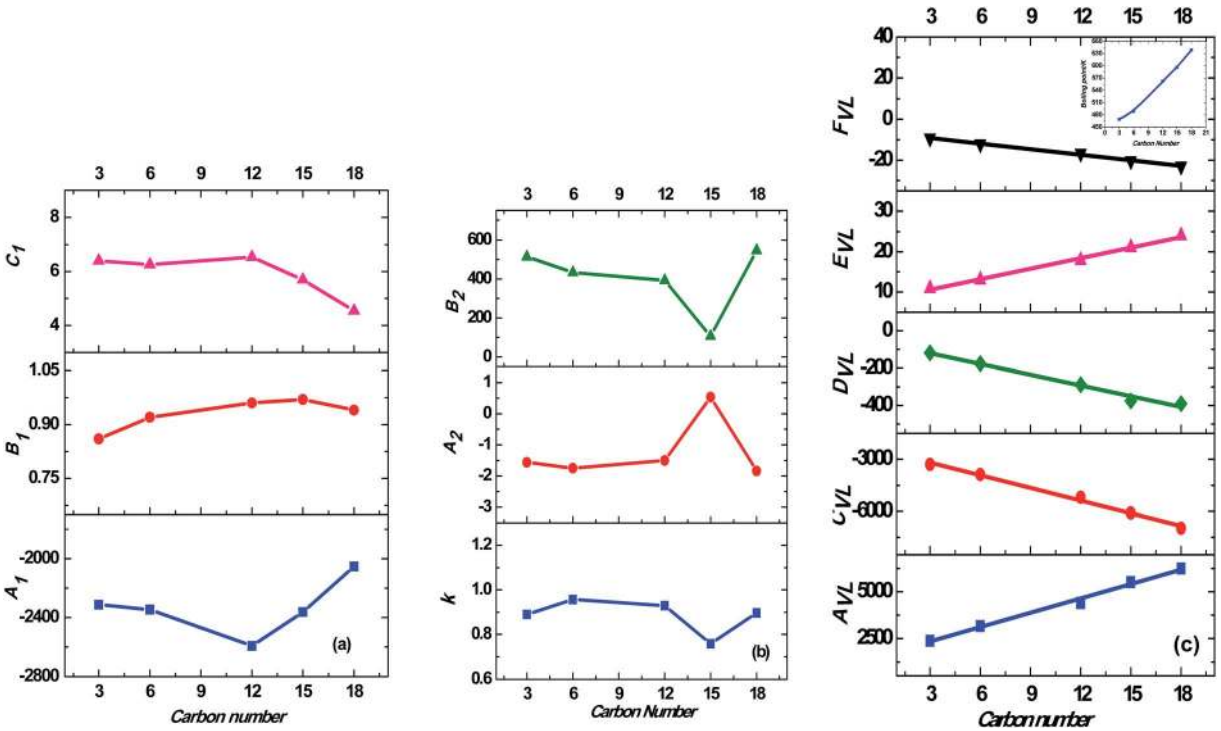

Fig. 7 Correlation of model parameters with carbon number of trialkyl phosphates; (a) MT model (eqn (3)); model parameters are represented by the symbols, ■, A_1; ●, B_1; ▲, C_1; (b) Chrastil model (eqn (4)); model parameters are represented by the symbols, ■, k; ●, A_2; ▲, B_2; (c) association model based on van Laar activity coefficient model (eqn (7)); model parameters are represented by the symbols, ■, A_{VL}; ●, C_{VL}; ◆, D_{VL}; ▲, E_{VL}; ▼, F_{VL}. The inset of this figure represents the relation between carbon number and normal boiling point of the trialkyl phosphates.

of the trialkyl phosphate series as well as predict the solubilities of these compounds at different temperatures and pressures.

5. Conclusions

The solubilities of a series of trialkyl phosphates were determined in supercritical carbon dioxide ($SCCO_2$). All the trialkyl phosphates examined in the present study are highly soluble in $SCCO_2$ and can be employed as ligands in the SFE of metal ions. The solubility of trialkyl phosphates increases with the pressure at constant temperature and it decreases with the temperature in the investigated pressure range. At constant temperature and pressure, solubility of trialkyl phosphates decreases with increase in molecular weight. The experimental results were successfully correlated using MT model, Chrastil and an association model based on van Laar activity coefficient model. The least AARD% of 4% was obtained for the association model based on van Laar activity coefficient model. The model parameters of the association model (eqn (7)) followed a linear relationship with the carbon number (and boiling point) of the trialkyl phosphates and thus can be used to predict the solubilities of a homologous series of trialkyl phosphates.

Acknowledgements

The authors would like to thank M. Joseph, IGCAR for his constant encouragement and support. Giridhar Madras thanks the department of science and technology (DST), India for the J. C. Bose fellowship.

References

1 *Properties of supercritical fluids relevant to extraction and chromatography*, ed. A. A. Clifford, Harwood Academic Publishers, Amsterdam, 1999.
2 M. A. McHugh and V. J. Krukonis, *Supercritical fluid extraction: principles and practice*, Butterworth-Heinemann, Boston, MA, 2nd edn, 1994.
3 X. Zhang, S. Heinonen and E. Levänen, *RSC Adv.*, 2014, **4**, 61137–61152.
4 C. M. Wai, *Anal. Sci.*, 1995, **11**, 165–167.
5 K. E. Laintz, C. M. Wai, C. R. Yonker and R. D. Smith, *Anal. Chem.*, 1992, **64**, 2875–2878.
6 C. Erkey, *J. Supercrit. Fluids*, 2000, **17**, 259–287.
7 Y. Lin, N. G. Smart and C. M. Wai, *Trends Anal. Chem.*, 1995, **14**, 123–133.
8 L. L. Burger, *Nucl. Sci. Eng.*, 1963, **16**, 428–439.
9 T. H. Siddall, *Ind. Eng. Chem. Res.*, 1959, **51**, 41–44.
10 T. H. Siddall, *J. Inorg. Nucl. Chem.*, 1960, **13**, 151–155.
11 L. L. Burger, *J. Phys. Chem.*, 1958, **62**, 590–593.
12 P. R. V. Rao, *Miner. Process. Extr. Metall. Rev.*, 1998, **18**, 309–331.
13 *The purex process*, ed. H. A. C. Mckay, J. H. Miles and J. L. Swanson, CRC Press, Boca Raton, Florida, USA, 1990.

14 *The Thorex process*, ed. W. D. Bond, CRC Press, Boca Raton, Florida, USA, 1990.
15 A. Suresh, T. G. Srinivasan and P. R. V. Rao, *Solvent Extr. Ion Exch.*, 1994, **12**, 727–744.
16 A. Suresh, T. G. Srinivasan and P. R. V. Rao, *Solvent Extr. Ion Exch.*, 2009, **27**, 258–294.
17 B. Sreenivasulu, A. Suresh, S. Subramaniam, K. N. Sabharwal, N. Sivaraman, K. Nagarajan, T. G. Srinivasan and P. R. V. Rao, *Solvent Extr. Ion Exch.*, 2015, **33**, 120–133.
18 Y. Lin, R. D. Brauer, K. E. Laintz and C. M. Wai, *Anal. Chem.*, 1993, **65**(18), 2549–2551.
19 B. J. Mincher, R. V. Fox, R. G. G. Holmes, R. A. Robbins and C. Boardman, *Radiochim. Acta*, 2001, **89**, 613–617.
20 R. Kumar, N. Sivaraman, K. Sujatha, T. G. Srinivasan and P. R. V. Rao, *Radiochim. Acta*, 2007, **95**, 577–584.
21 R. Kumar, N. Sivaraman, E. S. Vadivu, T. G. Srinivasan and P. R. Vasudeva Rao, *Radiochim. Acta*, 2003, **91**, 197–201.
22 K. Sujatha, K. C. Pitchaiah, N. Sivaraman, T. G. Srinivasan and P. R. V. Rao, *Am. J. Anal. Chem.*, 2012, **3**, 916–922.
23 K. Sujatha, K. C. Pitchaiah, N. Sivaraman, K. Nagarajan, T. G. Srinivasan and P. R. V. Rao, *Desalin. Water Treat.*, 2013, **52**, 470–475.
24 K. C. Pitchaiah, K. Sujatha, C. V. S. B. Rao, S. Subramaniam, N. Sivaraman and P. R. V. Rao, *Radiochim. Acta*, 2015, **103**, 245–255.
25 H. S. Ghaziaskar and M. Kaboudvand, *J. Supercrit. Fluids*, 2008, **44**, 148–154.
26 R. B. Gupta and J.-J. Shim, *Solubility in supercritical carbon dioxide*, CRC Press, Boca Raton, Florida, 1st edn, 2006.
27 Y. Meguro, S. Iso, T. Sasaki and Z. Yoshida, *Anal. Chem.*, 1998, **70**, 774–779.
28 N. G. Smart, T. Carleson, T. Kast, A. A. Clifford, M. D. Burford and C. M. Wai, *Talanta*, 1997, **44**, 137–150.
29 C. M. Wai and S. Wang, *Anal. Chem.*, 1996, **68**, 3516–3519.
30 W. J. Schmitt and R. C. Reid, *Chem. Eng. Commun.*, 1988, **64**, 155–176.
31 S. J. Nejad, R. Mohammadikhah, H. Abolghasemi, M. A. Moosavian and M. G. Maragheh, *Can. J. Chem. Eng.*, 2009, **87**, 930–938.
32 H. S. Yeoh, G. H. Chong, N. M. Azahan, R. A. Rahman and T. S. Y. Choong, *Eng. J.*, 2013, **17**, 67–78.
33 A. N. Sarve, M. N. Varma and S. S. Sonawane, *RSC Adv.*, 2015, **5**, 69702–69713.
34 M. Li, X. Huang, H. Liu, B. Liu, Y. Wu and L. Wang, *RSC Adv.*, 2015, **5**, 45520–45527.
35 S. K. Jha and G. Madras, *Ind. Eng. Chem. Res.*, 2005, **44**, 7038–7041.
36 B. E. Poling, J. M. Prausnitz and J. P. O'Connell, *The properties of gases and liquids*, McGraw-Hill, New York, 5th edn, 2001.
37 D. M. Himmelblau, *Korean J. Chem. Eng.*, 2000, **17**, 373–392.
38 J. Chrastil, *J. Phys. Chem.*, 1982, **86**, 3016–3021.
39 Y. Adachi and B. C.-Y. Lu, *Fluid Phase Equilib.*, 1983, **14**, 147–156.
40 J. M. D. Valle and J. M. Aguilera, *Ind. Eng. Chem. Res.*, 1988, **27**, 1551–1553.
41 K. D. Bartle, A. A. Clifford, S. A. Jafar and G. F. Shilstone, *J. Phys. Chem. Ref. Data*, 1991, **20**, 713–757.
42 M. D. Gordillo, M. A. Blanco, A. Molero and E. M. D. L. Ossa, *J. Supercrit. Fluids*, 1999, **15**, 183–190.
43 J. Méndez-Santiago and A. S. Teja, *Fluid Phase Equilib.*, 1999, **158**, 501–510.
44 C. Garlapati and G. Madras, *Fluid Phase Equilib.*, 2009, **283**, 97–101.
45 C. Garlapati and G. Madras, *J. Chem. Thermodyn.*, 2010, **42**, 193–197.
46 X. Bian, Z. Du and Y. Tang, *Thermochim. Acta*, 2011, **519**, 16–21.
47 D. L. Sparks, R. Hernandez and L. A. Estévez, *Chem. Eng. Sci.*, 2008, **63**, 4292–4301.
48 R. C. Narayan, J. V. Dev and G. Madras, *J. Supercrit. Fluids*, 2015, **101**, 87–94.
49 N. Lamba, R. C. Narayan, J. Raval, J. Modak and G. Madras, *RSC Adv.*, 2016, **6**, 17772–17781.
50 N. Lamba, R. C. Narayan, J. Modak and G. Madras, *J. Supercrit. Fluids*, 2016, **107**, 384–391.
51 M. D. A. Saldaña, B. Tomberli, S. E. Guigard, S. Goldman, C. G. Gray and F. Temelli, *J. Supercrit. Fluids*, 2007, **40**, 7–19.
52 F. Temelli, *J. Supercrit. Fluids*, 2009, **47**, 583–590.
53 K. H. Kim and Y. Kim, *Bull. Korean Chem. Soc.*, 2007, **28**, 2454–2458.
54 S. K. Jha and G. Madras, *Fluid Phase Equilib.*, 2004, **225**, 59–62.
55 R. S. Edmundson, *Dictionary of organophosphorous compounds*, Chapman and Hall Ltd, New York, London, 1988.
56 K. Paneerselvam, M. P. Antony, T. G. Srinivasan and P. R. V. Rao, *Thermochim. Acta*, 2010, **511**, 107–111.